




Cite this: *Phys. Chem. Chem. Phys.*,
2018, 20, 1005

A density functional theory study of aldehydes and their atmospheric products participating in nucleation†

Xiangli Shi,^a Ruiming Zhang,^a Yanhui Sun,^b Fei Xu,^a Qingzhu Zhang ^{*a} and Wenxing Wang^a

Aldehydes have been speculated as important precursor species in the formation of new atmospheric particles. In the present work, quantum chemical calculations were performed to investigate the hydrogen bonding interaction and the Gibbs free energy of formation (ΔG) for clusters consisting of sulfuric acid and aldehydes as well as their atmospheric reaction products. Calculations were conducted at 298 K and 1 atm at the M06-2X/6-311+G(3df,3pd) level. The results show that the addition of aldehyde compounds to H_2SO_4 unlikely contributes to new particle formation. However, their products from aldol condensation, hydration, and polymerization reactions can promote new particle formation by stabilizing sulfuric acid in the first step of nucleation. Moreover, the favorability of the interaction in the absence of water between sulfuric acid and the addition products is as follows: the hydration products > aldol condensation > aldehydes, but the results may be changed if water molecules are added. In particular, the calculated ΔG values imply that the monohydrate of glyoxal is more likely to nucleate with H_2SO_4 in comparison with ammonia in the presence or absence of water.

Received 12th September 2017,
Accepted 5th December 2017

DOI: 10.1039/c7cp06226e

rsc.li/pccp

1. Introduction

New particle formation is one of the primary sources of atmospheric aerosols, which have received much attention as they can significantly influence the climate and human health.^{1–3} Nucleated particles include the formation of stabilized clusters and their subsequent growth. The size distribution of nanometer-scale particles and the concentrations of various species participating in particle nucleation can be directly detected in the atmosphere. However, the underlying mechanism of new particle formation remains poorly understood, especially for the nucleation producing particles with a mobility diameter of less than 2 nm.⁴ Sulfuric acid (SA) is a primary driver of atmospheric particle nucleation, of which a gaseous concentration of 10^6 – 10^7 molecules cm^{-3} or more is required for new particle formation.⁵ However, atmospheric measurements suggest that only one or two sulfuric acid molecules are present in the critical nucleus. Quantum chemical calculations predicted

that clusters containing only sulfuric acid (and water) need to be stabilized with amines, or ammonia.^{5–9} Although sulfuric acid, water, and simple compounds including ammonia and amines drive the first steps of atmospheric particle formation, their concentrations are not enough to explain the particle nucleation rates and growth rates.^{1,10,11} Organic compounds, as other nucleation candidates, play important roles in particle formation and the subsequent growth stages. Riipinen I. *et al.* suggested that organic compounds likely dominate the first steps of growth in particles with a diameter close to 1 nm, which are stabilized by sulfuric acid.¹²

Atmospheric aldehydes originate from anthropogenic and biogenic sources and the photochemical degradation of volatile organic compounds.¹³ In acidic solution, carbonyl compounds can participate in various reactions, such as hydration, polymerization, aldol condensation, hemiacetal/acetal formation, or cationic rearrangement.^{14,15} Atmospheric oxidation of aldehydes by OH radicals and other oxidants can form carboxylic acids to engage in aerosol formation.^{16–18} Similar to those reactions in aqueous solution, the products of aldehyde hydration, polymerization, and aldol condensation can contribute to particle growth in the atmosphere.^{1,19,20} With the presence of ammonium and carbonate ions in tropospheric aerosols, the aldol condensation between acetaldehyde and acetone could be as fast as that in concentrated sulfuric acid and likely competes with their reactions with OH radicals.²¹ In comparison with

^a Environment Research Institute, Shandong University, Jinan 250100, P. R. China.
E-mail: zqz@sdu.edu.cn; Fax: +86-531-8836 1990

^b College of Environment and Safety Engineering, Qingdao University of Science and Technology, Qingdao 266042, P. R. China

† Electronic supplementary information (ESI) available: Gibbs free energies, Cartesian coordinates of minimum structures and minimum-energy structures of single molecules calculated using M06-2X/6-311+G(3df,3pd). See DOI: 10.1039/c7cp06226e

simple carbonyls, α -dicarbonyls such as glyoxal and methylglyoxal are significantly more reactive in the particle nucleation processes *via* hydration reaction or aldol condensation.¹ Further investigation is required to delineate the mechanism of new particle formation and growth involving these products discussed above.

Formaldehyde (HCHO), acetaldehyde (CH₃CHO), and glyoxal (C₂H₂O₂) are the most common aldehydes in clouds, dew, and fogwater.^{22–27} Previous theoretical studies showed that hydration and polymerization of formaldehyde and acetaldehyde are not thermodynamically favorable under atmospheric conditions. However, it is feasible for formaldehyde and acetaldehyde to undergo aldol condensation. Glyoxal tends to participate in hydration and polymerization reactions.^{28,29} In addition, sulfuric acid and organic acid can serve as effective catalysts in promoting the hydration of formaldehyde and acetaldehyde.³⁰ Herein, quantum chemical calculations are employed to investigate the molecular interaction between sulfuric acid and the above compounds (formaldehyde, acetaldehyde, glyoxal, and their corresponding hydrates and oligomers) in order to fully understand their roles in the initial steps of particle nucleation in the atmosphere. Furthermore, the effect of water on the cluster formation is considered. The Gibbs free energy of formation (ΔG) is determined for the reaction of aldehydes as well as atmospheric reaction products with sulfuric acids using density functional theory (DFT) by implementing a three-consecutive-step process – Basin Hopping Monte Carlo (BHMC) conformational sampling, simulated annealing optimization, and subsequent geometry optimization and frequency calculations. The derived information provides new insights into the impact of aldehydes on sulfuric acid pre-nucleation clusters as well as their atmospheric implications. Quantum chemistry calculations and kinetics modeling were performed in this research using the Atmospheric Cluster Dynamics Code (ACDC) to probe the evaporation rates of clusters.

2. Computational methods

The starting chemical geometries for the investigated compounds were generated by Basin Hopping Monte Carlo (BHMC) conformational sampling. The BHMC simulation was performed using the Generalized Amber Force Field (GAFF) in the Amber program and simulated annealing optimization was conducted in the Ampac program using the semi-empirical PM6 method.^{31–33} The DFT calculations were carried out with the aid of the Gaussian 09 package.³⁴ The geometries of the isomers were optimized at the B3LYP/6-31g(d,p) level and their corresponding vibrational frequencies were computed at the same level. Both geometry optimization and frequency calculations were performed at 298 K and 1 atm. To identify the lowest free energy structure, we initially utilized BHMC simulation to generate original geometries. Subsequently, the obtained configurations were optimized using the simulated annealing method to produce more structures, which were subjected to manual selection for the lower-energy configurations. The manually selected configurations were

optimized at the B3LYP/6-31g(d,p) level for energy comparison. We next carried out the circulation including simulated annealing optimization and DFT calculations until the lowest-energy configurations identified from two circulations have an energy difference of <2 kcal mol^{−1}. Finally, the most stable configurations (within 3 kcal mol^{−1} of the identified isomer) were optimized and the frequencies were calculated at the M06-2X/6-31+G(d,p) level. Their corresponding zero-point energies (ZPEs) were determined at the M06-2X/6-311+G(3df,3pd) level. The M06-2X functional was chosen in the present calculations because it yields ΔG values and structural characteristics showing remarkable agreement with experiments and *ab initio* calculations.^{35–39}

We applied the thermodynamic data at the M06-2X/6-311+G(3df,3pd) level to complete the Atmospheric Cluster Dynamics Code (ACDC) simulations. The detailed theory of the ACDC was introduced in a study by McGrath *et al.*⁴⁰ In this dynamical model, the time-dependent cluster concentrations are solved by integrating numerically the differential equations using the ode15s solver with the MATLAB (R2017a) program. The simulated system is a “3 × 3 box”, where 3 is the maximum number of H₂SO₄ or P3 molecules in the clusters. The ACDC simulations were performed at 298.15 K. According to Zhang *et al.*, a constant coagulation sink coefficient of 2.5×10^{-3} s^{−1} was used for taking into account external losses.⁴¹ Moreover, the sulfuric acid concentration was set to be 10⁶ cm^{−3} (a value relevant to atmospheric nucleation) and the atmospheric P3 concentration was set to be 10 ppt (a hypothetical value) in the ACDC simulations.^{1,28–30}

3. Results and discussion

Recent theoretical research showed that the DFT functional M06-2X is reliable for determining structures and ΔG values of atmospheric molecular clusters.^{35,42,43} Although M06-2X may overestimate the binding energies, it is efficient to distinguish the trends of different cluster nucleation by evaluating ΔG values. To illustrate the validity of the currently utilized calculation method, we calculated the ΔG values of clusters composed of sulfuric acid (SA) and H₂O. As listed in Table 1, the calculations at the M06-2X/6-311+G(3df,3pd) level provide ΔG values that are in better agreement with experimental observations⁴⁴ in comparison with those obtained at the PW91PW91/6-311+G(2d,2p) level.^{45,46}

3.1 Aldehydes directly involved in nucleation

In order to elucidate the activity of different aldehydes in sulfuric acid nucleation, ΔG values were calculated for the addition of a H₂SO₄ molecule to aldehyde molecules including formaldehyde

Table 1 Comparison of Gibbs free energy (kcal mol^{−1}) of formation (ΔG) for the sulfuric acid–water complex calculated using the PW91PW91 and M06-2X methods with the experimental value⁴²

Reaction	PW91PW91/ 6-311+G(2d,2p)	M06-2X/ 6-311+G(3df,3pd)	Experiment value ⁴²
SA + W \rightleftharpoons SA–W	−2.09	−3.76	−3.6 \pm 1.0

cases of aldehydes. The identified most stable configurations (shown in Fig. 1) reveal that a hydrogen bond is formed between sulfuric acid and formaldehyde/acetaldehyde/butyraldehyde/octanal⁴⁷ and the hydrogen bond lengths have negligible differences among the four cases. As shown in Table 2, the ΔG values

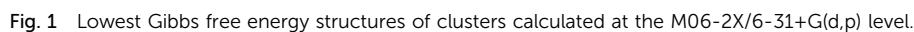


Table 2 Gibbs free energies of formation (ΔG) for clusters composed of atmospheric precursors (sulfuric acid, other common nucleation candidates, and aldehydes) calculated at 298 K and 1 atm

Reactions	ΔG (kcal mol ⁻¹)
SA + NH ₃ \rightleftharpoons SA-NH ₃	-7.38
SA + SUA \rightleftharpoons SA-SUA	-11.33
SA + DMA \rightleftharpoons SA-DMA	-13.27
SA + SA \rightleftharpoons SA-SA	-10.21
SA + HCHO \rightleftharpoons SA-HCHO	-2.50
SA + CH ₃ CHO \rightleftharpoons SA-CH ₃ CHO	-3.74
SA + CH ₃ CHO \rightleftharpoons SA-CH ₃ CHO	-4.14
SA + CH ₃ CHO \rightleftharpoons SA-CH ₃ CHO	-4.22
SA + (CHO) ₂ \rightleftharpoons SA-(CHO) ₂	-0.73

of the addition of H₂SO₄ to the aldehydes range from -2.4 to -4.5 kcal mol⁻¹, which are much smaller than those determined for the reactions between H₂SO₄ and ammonia/succinic acid/dimethylamine/sulfuric acid. Thus, aldehydes have negligible capability to stabilize sulfuric acid in the early stages of new particle formation. In addition, the ΔG value (shown in Table 2) calculated for the reaction between formaldehyde and ammonia indicates that it is unlikely that small gaseous aldehydes enhance nucleation by interacting with ammonia. Therefore, small gaseous aldehydes with a carbonyl group have no direct contribution to the formation of atmospheric particle nucleation, which is consistent with the previous experimental observation.²⁸ The experiments conducted using nano-TDMA reported that H₂SO₄ nanoparticles showed noticeable growth with exposure to glyoxal (C₂H₂O₂).⁴⁸ However, a ΔG value of 0.7 kcal mol⁻¹ was determined for the formation of a (H₂SO₄)(C₂H₂O₂) complex containing a hydrogen bond. This suggests that glyoxal likely participates in the atmospheric particle nucleation through other processes such as hydration, polymerization, and aldol condensation reactions.

3.2 Aldol condensation in nucleation

Previous studies showed that aldol condensation of aldehydes contributes to atmospheric particle growth and the majority of the carbonyl compounds are capable of undergoing aldol condensation in the atmosphere.^{1,49} In order to evaluate the roles of aldehyde aldol condensation in the first steps of particle nucleation, theoretical calculations were performed for systems where sulfuric acid reacts with 3-hydroxybutyraldehyde and 2-butanal, which are the products of acetaldehyde *via* aldol condensation and dehydration. The identified conformations with the lowest G values of 3-hydroxybutyraldehyde (P1) and 2-butanal (P2) are presented in Fig. 1. An intramolecular hydrogen bond is observed in 3-hydroxybutyraldehyde. Compared with the formation of a (SA)(CH₃CHO) cluster, the formation of (SA)(P1) and (SA)(P2) clusters (shown in Fig. 1) is observed to be significantly more favorable with ΔG values of -5.28 and -4.74 kcal mol⁻¹. Both 3-hydroxybutyraldehyde and 2-butanal are able to form a hydrogen bond with sulfuric acid. This implies that the aldol condensation products of aldehydes are more likely to directly participate in atmospheric particle nucleation.

To further investigate the viewpoint above, we studied the trend of (SA)(P1) cluster growth by adding another molecule,

Table 3 Gibbs free energies of formation (ΔG) for clusters composed of atmospheric precursors (sulfuric acid and aldehyde products from aldol condensation) calculated at 298 K and 1 atm

Reactions	ΔG (kcal mol ⁻¹)
SA + P1 \rightleftharpoons SA-P1	-5.28
SA + P2 \rightleftharpoons SA-P2	-4.74
SA-P1 + SA \rightleftharpoons 2SA-P1	-12.78
SA-P1 + P1 \rightleftharpoons SA-2P1	-4.17
SA-P1 + DMA \rightleftharpoons SA-P1-DMA	-15.08
P1 + H ₂ O \rightleftharpoons P1-H ₂ O	2.92
P1 + DMA \rightleftharpoons P1-DMA	1.23
P1 + SUA \rightleftharpoons P1-SUA	-3.10
P1 + P1 \rightleftharpoons 2P1	2.59

sulfuric acid, 3-hydroxybutyraldehyde (P1), or dimethylamine (DMA), to this cluster. The corresponding conformations with the lowest Gibbs free energy values and ΔG values calculated at 298 K are shown in Fig. 1 and Table 3. The ΔG values imply that the formation of a (SA)(P1)(DMA) cluster is much more energetically favored than the formation of (2SA)(P1) and (SA)(2P1). In addition, the formation of a (SA)(2P1) cluster is more restricted than the case of a (SA)(P1) cluster as the two P1 molecules in the (SA)(2P1) cluster prevent SA from forming a hydrogen bond with other molecules. The ΔG values of -15.08 kcal mol⁻¹ and -12.78 kcal mol⁻¹ are determined for the addition of SA and dimethylamine to the (SA)(P1) cluster, respectively. In comparison, the addition of SA or dimethylamine to a single SA molecule is less favorable, exhibiting ΔG values of -13.27 kcal mol⁻¹ and -10.21 kcal mol⁻¹, respectively. This is likely due to the condensation of low-volatility P1 reducing the surface tension of SA in atmospheric particle nucleation.⁴

We further explored the possibility of forming a complex between P1 and H₂O or dimethylamine (DMA) or succinic acid (SUA) or a second P1. The ΔG values of the corresponding cluster are shown in Table 3. The results imply that P1 presents weak interaction with H₂O, dimethylamine, or a second P1, possessing positive ΔG in all cases. Although the formation of P1-SUA has a ΔG of -3.10 kcal mol⁻¹, it is not energetically favorable to form (P1)(SUA).

Overall, the calculations presented above illustrate that aldol condensation products of aldehydes participate in the first steps of atmospheric particle nucleation by stabilizing SA or interacting with organic acids. In addition, the calculated ΔG values for various clusters imply that the aldol condensation products of aldehydes in the absence of water exhibit less capability to stabilize sulfuric acid than the common nucleation precursors such as NH₃, (CH₃)₂NH, and H₂SO₄. Thus, the aldol condensation products of aldehydes are unlikely the key species in the first steps of atmospheric particle nucleation and aldol condensation is a plausible route contributing to particle growth if there is no water molecule.

3.3 Hydration of aldehydes

Glyoxal (HCOCHO) is significantly more reactive than simple carbonyls. A number of previous studies have reported that glyoxal can directly promote atmospheric particle nucleation.¹ The reaction between glyoxal and water to produce glyoxal-diol

(HCOCH(OH)₂) (monohydrate of glyoxal) competes with the reaction involving HCOCHO and OH under certain atmospheric conditions.⁵⁰ The role of glyoxal in atmospheric particle nucleation remains unclear.

Glyoxal undergoes hydration and its hydrate subsequently promotes self- and cross-oligomerization to produce dimmers, trimers, and polymers, as shown in Fig. 1. We selected glyoxal, glyoxal monohydrate (P3), glyoxal dehydrate (P4), and the polymer of two glyoxal dehydrate (P5) to probe their interaction with sulfuric acid possibly occurring in the first steps of atmospheric particle nucleation. Two hydrogen bonds exist in both the (P3)(H₂SO₄) and (P4)(H₂SO₄) clusters, whereas three hydrogen bonds are present in the P5–H₂SO₄ cluster. Our calculations show that the formation of a cluster between glyoxal and one sulfuric acid molecule has a ΔG value of -0.73 kcal mol⁻¹. In contrast, P3, P4, and P5 form clusters with one sulfuric acid molecule with the ΔG values of -8.30 , -7.17 , and -7.30 kcal mol⁻¹, respectively. This implies that hydrates of glyoxal are more energetically favored to form hydrogen bonds with sulfuric acid and, particularly, the ΔG value of the (P3)(H₂SO₄) cluster is higher than that of the (NH₃)(H₂SO₄) cluster.

Calculations are further performed for the (P3)(H₂SO₄) cluster with increasing number of glyoxal monohydrate (P3) and sulfuric acid molecules added on in order to elucidate its growth mechanism. The formation of (P3)₂(H₂SO₄) and (P3)₃(H₂SO₄) clusters by adding P3 to the (P3)(H₂SO₄) cluster is determined to have ΔG values of -5.09 kcal mol⁻¹ and -2.96 kcal mol⁻¹, respectively. Similarly, -7.00 and -7.91 kcal mol⁻¹ are found for the ΔG values of (P3)(H₂SO₄)₂ and (P3)(H₂SO₄)₃ cluster formation, respectively, fulfilled by adding sulfuric acid molecules to a (P3)(H₂SO₄) cluster. These calculations suggest that glyoxal hydrates unlikely serve as the key species in the first steps in atmospheric particle nucleation; however, they are capable of stabilizing sulfuric acid to promote the nucleation process. It also noted that a single sulfuric acid molecule was likely insufficient to assist further particle growth.

Sulfuric acid and organic acids are effective catalysts promoting the hydration of formaldehyde and acetaldehyde.³⁰ Herein, monohydrates of formaldehyde (P6) and acetaldehyde (P7) are investigated to elucidate their ability to react with sulfuric acid. The configurations and ΔG of (P6)(H₂SO₄) cluster and (P7)(H₂SO₄) cluster are displayed in Fig. 1 and Table 4, respectively. Two hydrogen bonds are observed for both of the two clusters. In addition, the formation of a (P6)(H₂SO₄) cluster and (P7)(H₂SO₄) cluster has a ΔG of -5.91 kcal mol⁻¹ and -5.69 kcal mol⁻¹, respectively, which are 2–3 kcal mol⁻¹ higher than those of the (P3)(H₂SO₄) cluster, (P4)(H₂SO₄) cluster, and (P5)(H₂SO₄) cluster. These observations imply that glyoxal hydrates are significantly more reactive than simple carbonyl hydrates.

3.4 Nucleation in the presence of water

To study the effect of water on the above nucleation involving products of aldehydes, we chose SA, P1, P3, and P4 nucleating with one to two water molecules to compare with the case in the absence of water. The configurations and ΔG values of the

Table 4 Gibbs free energies of formation (ΔG) for clusters composed of atmospheric precursors (sulfuric acid and hydrates of aldehydes) calculated at 298 K and 1 atm

Reactions	ΔG (kcal mol ⁻¹)
SA + P3 \rightleftharpoons SA–P3	–8.30
SA + P4 \rightleftharpoons SA–P4	–7.17
SA + P5 \rightleftharpoons SA–P5	–7.30
SA–P3 + P3 \rightleftharpoons SA–2P3	–5.09
SA–2P3 + SA \rightleftharpoons 2SA–2P3	–3.72
SA–2P3 + P3 \rightleftharpoons SA–3P3	–2.96
SA–P3 + SA \rightleftharpoons 2SA–P3	–7.00
2SA–P3 + P3 \rightleftharpoons 2SA–2P3	–1.81
2SA–P3 + SA \rightleftharpoons 3SA–P3	–7.91
SA + P6 \rightleftharpoons SA–P6	–5.91
SA + P7 \rightleftharpoons SA–P7	–5.69

Table 5 Gibbs free energies of formation (ΔG) for clusters composed of atmospheric precursors (sulfuric acid and aldehyde products from aldol condensation as well as hydrates of aldehydes in the presence of water) calculated at 298 K and 1 atm

Reactions	ΔG (kcal mol ⁻¹)
SA–H ₂ O + H ₂ O \rightleftharpoons SA–2H ₂ O	–2.05
SA–H ₂ O + NH ₃ \rightleftharpoons SA–NH ₃ –H ₂ O	–5.87
SA–NH ₃ + H ₂ O \rightleftharpoons SA–NH ₃ –H ₂ O	–2.25
SA–H ₂ O + P1 \rightleftharpoons SA–P1–H ₂ O	–6.83
SA–P1 + H ₂ O \rightleftharpoons SA–P1–H ₂ O	–5.31
SA–P1–H ₂ O + H ₂ O \rightleftharpoons SA–P1–2H ₂ O	2.76
SA–2H ₂ O + P1 \rightleftharpoons SA–P1–2H ₂ O	–2.02
SA–P1–H ₂ O + SA \rightleftharpoons 2SA–P1–H ₂ O	–10.10
2SA–P1 + H ₂ O \rightleftharpoons 2SA–P1–H ₂ O	–2.63
SA–H ₂ O + P3 \rightleftharpoons SA–P3–H ₂ O	–6.41
SA–P3 + H ₂ O \rightleftharpoons SA–P3–H ₂ O	–1.87
SA–H ₂ O + P4 \rightleftharpoons SA–P4–H ₂ O	–5.14
SA–P4 + H ₂ O \rightleftharpoons SA–P4–H ₂ O	–1.74

corresponding cluster are shown in Table 5. As displayed in Tables 3–5, the Gibbs free energy associated with the formation of (SA)(P1)(H₂O) from (SA)(H₂O) and P1 (-6.83 kcal mol⁻¹) is more negative than the Gibbs free energy of (SA)(P1) formation from SA and P1 (-5.28 kcal mol⁻¹), but the Gibbs free energy associated with the formation of (SA)(P3)(H₂O) and (SA)(P4)(H₂O) from (SA)(H₂O), P3 and P4 (-6.41 and -5.14 kcal mol⁻¹, respectively) is less negative than that of (SA)(P3) and (SA)(P4) formation from SA, P3 and P4 (-8.30 and -7.17 kcal mol⁻¹, respectively). Similar relations are observed in the formation of (SA)(P1)(H₂O), (SA)(P3)(H₂O) and (SA)(P4)(H₂O) from (SA)(P1), (SA)(P3), (SA)(P4) and H₂O in comparison with the formation of (SA)(H₂O) from SA and H₂O. Furthermore, the calculated values of ΔG indicate that the formation of (SA)(P1)(H₂O) and (SA)(P3)(H₂O) from (SA)(H₂O), P1 and P3 is more favored than the formation of (SA)(NH₃)(H₂O) from (SA)(H₂O) and NH₃.

We further investigate the growth processes of P1 nucleating with SA in the presence of water. As shown in Table 5, adding another water molecule to a (SA)(P1)(H₂O) cluster (2.76 kcal mol⁻¹) to form a (SA)(P1)(H₂O)₂ cluster is infeasible, whereas adding another SA molecule to a (SA)(P1)(H₂O) cluster (-10.10 kcal mol⁻¹) to form a (SA)₂(P1)(H₂O) cluster is more viable. These observations imply that the products of aldehydes possibly play nonnegligible roles in new particle formation in the presence of water.

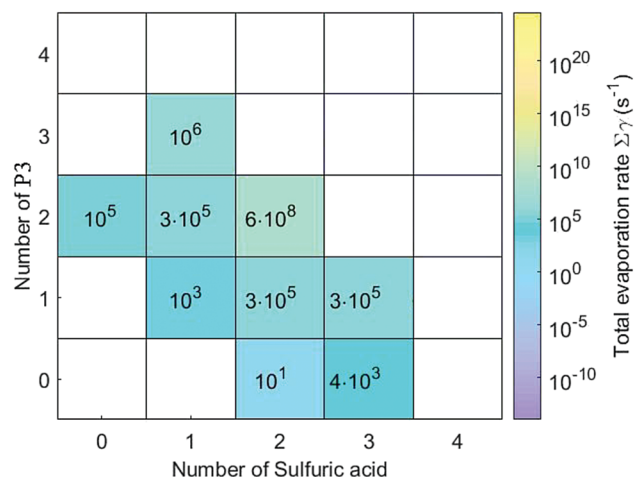


Fig. 2 Evaporation rates for $(\text{SA})_m(\text{P3})_n$ on the SA–P3 grid at 298.15 K.

3.5 Evaporation rates

Taking into consideration the computational cost, we studied the initially sectional SA–P3 cluster growth in the absence of water. The obtained evaporation rates are used to evaluate the stability of clusters at the given concentration of reactions. The evaporation rates for $(\text{SA})_m(\text{P3})_n$ ($m = 1-3$ and $n = 1-3$) on the SA–P3 grid at 298.15 K are presented in Fig. 2. It shows that the evaporation rates for clusters $(\text{SA})_2$, $(\text{SA})(\text{P3})$, and $(\text{SA})_3$ are on the order of 10^{-10} – 10^{-3} s^{-1} , which are much smaller than those of other clusters shown in the grid. In addition, the evaporation rate of $(\text{SA})_2(\text{P3})_2$ is much higher than that of $(\text{SA})(\text{P3})_2$, $(\text{SA})(\text{P3})_3$, and $(\text{SA})_3(\text{P3})$, indicating that the $(\text{SA})_2(\text{P3})_2$ cluster is unlikely present in the growth routes.

4. Conclusions

We used DFT methods to elucidate the possibility of aldehydes as well as their products of aldol condensation, hydration, and polymerization reactions forming clusters with sulfuric acid in atmospheric particle formation. Geometries and ΔG values calculated at 298 K and 1 atm show that the products derived from the aldol condensation, hydration, and polymerization reactions of aldehydes likely participate in the initial steps of atmospheric particle nucleation and contribute to particle growth by stabilizing sulfuric acid. Structural analyses reveal that the number of hydrogen bonds is not in proportion with the values of ΔG . The presence of water can also affect the mechanism of new particle formation. In addition, small aldehydes directly involved in the nucleation exhibit a negligible effect for new particle formation. The studies of the formation pathways, steady-state concentrations, and formation rates of bigger clusters under different humidities are currently ongoing in our laboratory. Furthermore, it is also important to understand how the products of carbonyl compounds in the atmosphere participate in nucleation, which is an interesting topic for future studies.

Conflicts of interest

There are no conflicts to declare.

Acknowledgements

The work is financially supported by NSFC (National Natural Science Foundation of China, project no. 21337001, 21677089, 21407096) and Independent Innovation Foundation of Shandong University (IIFSDU, project no. 2017JC033).

References

- 1 R. Zhang, A. Khalizov, L. Wang, M. Hu and W. Xu, *Chem. Rev.*, 2012, **112**, 1957–2011.
- 2 R. Zhang, I. Suh, J. Zhao, D. Zhang, E. C. Fortner, X. Tie, L. T. Molina and M. J. Molina, *Science*, 2004, **304**, 1487–1490.
- 3 R. Zhang, *Science*, 2010, **328**, 1366–1367.
- 4 M. Kulmala, J. Kontkanen, H. Junninen, K. Lehtipalo, H. E. Manninen, T. Nieminen, T. Petäjä, M. Sipilä, S. Schobesberger, P. Rantala, A. Franchin, T. Jokinen, E. Järvinen, M. Äijälä, J. Kangasluoma, J. Hakala, P. P. Aalto, P. Paasonen, J. Mikkilä, J. Vanhanen, J. Aalto, H. Hakola, U. Makkonen, T. Ruuskanen, R. L. Mauldin III, J. Duplissy, H. Vehkamäki, J. Bäck, A. Kortelainen, I. Riipinen, T. Kurtén, M. V. Johnston, J. N. Smith, M. Ehn, T. F. Mentel, K. E. J. Lehtinen, A. Laaksonen, V. Kerminen and D. R. Worsnop, *Science*, 2013, **339**, 943–946.
- 5 P. H. McMurry, M. A. Fink, H. Sakurai and J. B. Nowak, *J. Geophys. Res.*, 2005, **110**, 2935–2948.
- 6 T. Kurtén, V. Loukonen, H. Vehkamäki and M. Kulmala, *Atmos. Chem. Phys.*, 2008, **8**, 7455–7476.
- 7 J. Kirkby, J. Curtius, J. Almeida, E. Dunne, J. Duplissy, S. Ehrhart, A. Franchin, S. Gagné, L. Ickes, A. Kürten, A. Kupe, A. Metzger, F. Riccobono, L. Rondo, S. Schobesberger, G. Tsagkogeorgas, D. Wimmer, A. Amorim, F. Bianchi, M. Breitenlechner, A. David, J. Dommen, A. Downard, M. Ehn, R. C. Flagan, S. Haider, A. Hansel, D. Hauser, W. Jud, H. Junninen, F. Kreissl, A. Kvashin, A. Laaksonen, K. Lehtipalo, J. Lima, E. R. Lovejoy, V. Makhmutov, S. Mathot, J. Mikkilä, P. Minginette, S. Mogo, T. Nieminen, A. Onnela, P. Pereira, T. Petäjä, R. Schnitzhofer, J. H. Seinfeld, M. Sipilä, Y. Stozhkov, F. Stratmann, A. Tomé, J. Vanhanen, Y. Viisanen, A. Virtala, P. E. Wagner, H. Walther, E. Weingartner, H. Wex, P. M. Winkler, K. S. Carslaw, D. R. Worsnop, U. Baltensperger and M. Kulmala, *Nature*, 2011, **476**, 429–433.
- 8 V. Loukonen, T. Kurtén, I. K. Ortega, H. Vehkamäki, A. A. H. Padua, K. Sellegri and M. Kulmala, *Atmos. Chem. Phys.*, 2010, **10**, 4961–4974.
- 9 P. Paasonen, T. Olenius, O. Kupiainen and T. Kurtén, *Atmos. Chem. Phys.*, 2012, **12**, 11485–11537.
- 10 I. Riipinen, J. R. Pierce, T. Yli-Juuti, T. Nieminen, S. Häkkinen, M. Ehn, H. Junninen, K. Lehtipalo, T. Petäjä, J. Slowik, R. Chang, N. C. Shantz, J. Abbatt, W. R. Leitch, V.-M. Kerminen, D. R. Worsnop, S. N. Pandis, N. M. Donahue and M. Kulmala, *Atmos. Chem. Phys.*, 2011, **11**, 3865–3878.
- 11 C. Kuang, I. Riipinen, S. L. Sihto and M. Kulmala, *Atmos. Chem. Phys.*, 2010, **10**, 8469–8480.
- 12 I. Riipinen, T. Ylijuuti, J. R. Pierce, T. Petäjä, D. R. Worsnop, M. Kulmala and N. M. Donahue, *Nat. Geosci.*, 2012, **5**, 453–458.

- 13 J. H. Seinfeld and S. N. Pandis, *Atmospheric chemistry and physics: from air pollution to climate change*, 2nd edn, John Wiley & Sons, Hoboken, New Jersey, 2006.
- 14 D. Barton and W. D. Ollis, *Comprehensive organic chemistry: the synthesis and reactions of organic compounds*, 1st edn, Pergamon Press, Oxford, New York, 1979.
- 15 F. A. Carey and R. J. Sundberg, *Advanced organic chemistry*, 4th edn, Kluwer Academic/Plenum Publishers, New York, 2000.
- 16 B. Ervens, B. J. Turpin and R. J. Weber, *Atmos. Chem. Phys.*, 2011, **11**, 11069–11102.
- 17 A. G. Carlton, B. J. Turpin, K. E. Altieri, S. Seitzinger, A. Reff, H.-J. Lim and B. Ervens, *Atmos. Environ.*, 2007, **41**, 7588–7602.
- 18 M. J. Perri, S. Seitzinger and B. J. Turpin, *Atmos. Environ.*, 2009, **43**, 1487–1497.
- 19 M. Jang and R. M. Kamens, *Environ. Sci. Technol.*, 2001, **35**, 4758–4766.
- 20 L. N. Hawkins, M. J. Baril, N. Sedehi, M. M. Galloway, D. O. D. Haan, G. P. Schill and M. A. Tolbert, *Environ. Sci. Technol.*, 2014, **48**, 2273–2280.
- 21 B. Nozière, P. Dziedzic and A. Córdova, *Phys. Chem. Chem. Phys.*, 2010, **12**, 3864–3872.
- 22 K. Matsumoto, S. Kawai and M. Igawa, *Atmos. Environ.*, 2005, **39**, 7321–7329.
- 23 M. Igawa, J. W. Munger and M. R. Hoffmann, *Environ. Sci. Technol.*, 1989, **23**, 556–561.
- 24 J. W. Munger, D. J. Jacob, B. C. Daube, L. W. Horowitz, W. C. Keene and B. G. Heikes, *J. Geophys. Res.*, 1995, **100**, 9325–9333.
- 25 J. L. Collett Jr., B. C. Daube, D. Gunz and M. R. Hoffmann, *Atmos. Environ.*, 1990, **24**, 1741–1757.
- 26 D. V. Pinxteren, A. Plewka, D. Hofmann, K. Müller, H. Kramberger, B. Svrčina, K. Bachmann, W. Jaeschke, S. Meters and J. L. Collett Jr., *Atmos. Environ.*, 2005, **39**, 4305–4320.
- 27 S. Steinberg and I. R. Kaplan, *Int. J. Environ. Anal. Chem.*, 1984, **18**, 253–266.
- 28 K. C. Barsanti and J. F. Pankow, *Atmos. Environ.*, 2004, **38**, 4371–4382.
- 29 K. C. Barsanti and J. F. Pankow, *Atmos. Environ.*, 2005, **39**, 6597–6607.
- 30 H. A. Rypkema, A. Sinha and J. S. Francisco, *J. Phys. Chem. A*, 2015, **119**, 4581–4588.
- 31 S. Kirkpatrick, C. D. Gelatt Jr. and M. P. Vecchi, *Science*, 1983, **220**, 606–615.
- 32 Z. Li and H. A. Scheraga, *Proc. Natl. Acad. Sci. U. S. A.*, 1987, **84**, 6611–6615.
- 33 J. P. K. Doye and D. J. Wales, *Phys. Rev. Lett.*, 1998, **80**, 1357–1360.
- 34 M. Frisch, G. Trucks, H. B. Schlegel, G. Scuseria, M. Robb, J. Cheeseman, G. Scalmani, V. Barone, B. Mennucci and G. A. Petersson, *Gaussian 09, revision A.02*, Gaussian Inc., Wallingford, CT, 2009, vol. 270, p. 271.
- 35 J. Elm, M. Bilde and K. V. Mikkelsen, *J. Chem. Theory Comput.*, 2012, **8**, 2071–2077.
- 36 J. Elm, M. Bilde and K. V. Mikkelsen, *Phys. Chem. Chem. Phys.*, 2013, **15**, 16442–16445.
- 37 H. R. Leverentz, J. I. Siepmann, D. G. Truhlar, V. Loukonen and H. Vehkamäki, *J. Phys. Chem. A*, 2013, **117**, 3819–3825.
- 38 A. B. Nadykto, H. Du and F. Yu, *Vib. Spectrosc.*, 2007, **44**(2), 286–296.
- 39 T. Kurtén, L. Torpo, C.-G. Ding, H. Vehkamäki, M. R. Sundberg, K. Laasonen and M. Kulmala, *J. Geophys. Res.*, 2007, **112**, 1407–1413.
- 40 M. J. McGrath, T. Olenius, I. K. Ortega, V. Loukonen, P. Paasonen, T. Kurten, M. Kulmala and H. Vehkama, *Atmos. Chem. Phys.*, 2012, **12**, 2345–2355.
- 41 H. Zhang, O. Kupiainen-Maatta, X. Zhang, V. Molinero, Y. Zhang and Z. Li, *J. Chem. Phys.*, 2017, **146**, 143–176.
- 42 N. Bork, L. Du and H. G. Kjaergaard, *J. Phys. Chem. A*, 2014, **118**, 1384–1389.
- 43 N. Bork, L. Du, H. Reimen, T. Kurten and H. G. Kjaergaard, *J. Phys. Chem. A*, 2014, **118**, 5316–5322.
- 44 D. R. Hanson and F. L. Eisele, *J. Phys. Chem. A*, 2000, **104**, 1715–1719.
- 45 W. Xu and R. Zhang, *J. Phys. Chem. A*, 2012, **116**, 4539–4550.
- 46 W. Xu and R. Zhang, *J. Chem. Phys.*, 2013, **139**, 064312.
- 47 P. Gilli, V. Bertolasi, V. Ferretti and G. Gilli, *J. Am. Chem. Soc.*, 1994, **116**, 909–915.
- 48 L. Wang, A. F. Khalizov, J. Zheng, W. Xu, Y. Ma, V. Lal and R. Zhang, *Nat. Geosci.*, 2010, **3**, 238–242.
- 49 B. Nozière and W. Esteve, *Atmos. Environ.*, 2007, **41**, 1150–1163.
- 50 M. Huang, S. Cai, Y. Liao, W. Zhao, C. Hu, Z. Wang and W. Zhang, *Chin. J. Chem. Phys.*, 2016, **29**, 335–343.